High resolution thermal remote sensing and the limits of species' tolerance

Gabrielle Ednie [Corresp., 1], **Jeremy T Kerr** [1]

[1] Department of Biology, University of Ottawa, Ottawa, Ontario, Canada

Corresponding Author: Gabrielle Ednie
Email address: gedni049@uottawa.ca

Extinction risks for many insect species, particularly across very broad spatial extents, have been linked to the growing frequency and severity of temperatures that exceed the boundaries of their realized niches. Measurement and mitigation of such impacts is hindered by the availability of high-resolution measurements of species-specific severity of extreme weather, especially temperature. While techniques enabling interpolation of broad-scale remote sensing metrics are vital for such efforts, direct remote sensing measurements of thermal conditions could ~~inform~~ improve habitat management by providing detailed insights that interpolative approaches cannot. Advances in unmanned aerial vehicle (UAV) technology have created opportunities to better evaluate the role of microclimates in local species extinctions. Here, we develop a method to create high-resolution maps of microclimates using UAV and thermal imaging technology that use species' realized niche boundaries to assess potential effects of severity of extreme temperatures. We generated air temperature maps (5cm resolution) and canopy height models (~~CHM;~~ 1cm resolution) for 15 sites in a rare alvar ecosystem in eastern Ontario. We validated these remote sensing observations against independent, *in situ* temperature observations using iButtons. Temperature observations were accurate and related to physical heterogeneity in alvar habitats. We converted temperature measures into estimates of proximity of thermal niche boundaries for three butterfly species found during field surveys. This is the first time that this method has been applied to high resolution remote sensing observations and offers potential to assess the availability and adequacy of microclimates within habitats at resolutions relevant for conservation management.

High resolution thermal remote sensing and the limits of species' tolerance

Gabrielle Ednie*[1]. and Jeremy T. Kerr[1]

[1] Biology Department, University of Ottawa, Ontario, Canada, K1N 6N5

*corresponding author:
Gabrielle Ednie[1]
Marie-Curie Private, Ottawa, Ontario, K1N 9B4, Canada
gedni049@uottawa.ca

Abstract

Extinction risks for many insect species, particularly across very broad spatial extents, have been linked to the growing frequency and severity of temperatures that exceed the boundaries of their realized niches. Measurement and mitigation of such impacts is hindered by the availability of high-resolution measurements of species-specific severity of extreme weather, especially temperature. While techniques enabling interpolation of broad-scale remote sensing metrics are vital for such efforts, direct remote sensing measurements of thermal conditions could ~~inform~~ improve habitat management by providing detailed insights that interpolative approaches cannot. Advances in unmanned aerial vehicle (UAV) technology have created opportunities to better evaluate the role of microclimates in local species extinctions. Here, we develop a method to create high-resolution maps of microclimates using UAV and thermal imaging technology that use species' realized niche boundaries to assess potential effects of severity of extreme temperatures. We generated air temperature maps (5cm resolution) and canopy height ~~models~~ (~~CHM;~~ 1cm resolution) for 15 sites in a rare alvar ecosystem in eastern Ontario. We validated these remote sensing observations against independent, *in situ* temperature observations using iButtons. Temperature observations were accurate and related to physical heterogeneity in alvar habitats. We converted temperature measures into estimates of proximity of thermal niche boundaries for three butterfly species found during field surveys. This is the first time that this method has been applied to high resolution remote sensing observations and offers potential to assess the availability and adequacy of microclimates within habitats at resolutions relevant for conservation management.

Introduction

Climate change exposes species to abiotic conditions that may exceed their tolerances (Kerr et al. 2015; Urban et al. 2016), leading to growing frequencies and severities of extreme weather events (Harris et al. 2018; Kerr 2020). Such changes contribute to the declines of many species (Riddell et al. 2021; Soroye et al. 2020). Over broad geographical areas, such extreme events are increasing extinction risks for populations of key pollinator species (Soroye et al. 2020) and vertebrates at global extents (Williams and Newbold, 2021). Distinguishing between effects of "press" events (e.g. shifts in average climatic conditions that can progressively change the suitability of an environment for particular species) vs. "pulse" events (e.g. short duration extreme weather that can cause population decline; Harris et al. 2018), temperature extremes ("pulse" events) in particular have been linked to changes in species colonization-extinction dynamics, contributing to declines for many species across broad geographical areas. Translating broad-scale models to direct local measurements that assess species' exposures to extreme temperature, relative to their individual tolerances, could improve habitat management and species' conservation prospects.

Microclimate refugia are areas where species can find shelter from extreme weather (Rull 2009). The size of these refugia depends on the body size and niche boundaries of each species (Keppel et al. 2012). Species distribution models (SDMs) are often used to forecast impacts of climate change on species' ranges (Algar et al. 2009; Kharouba et al. 2009; Porfirio et al. 2014). However, such methods rely heavily on long term climate data and are more appropriate for use at large biogeographical extents (Anderson & Gaston 2013; Ashcroft 2010; Potter et al. 2013). Species experience temperatures at very localized spatial extents (Suggitt et al. 2011). While some studies have measured microclimatic variation of complex local landscapes at scales relevant to the movement and habitat use of individual organisms, fewer studies have assessed this microclimatic variability relative to individual species' thermal boundaries comprehensively throughout habitats (Milling et al. 2018; Pincebourde et al. 2016; Rebaudo et al. 2016; Slavich et al. 2014; Suggitt et al. 2011; Suggitt et al. 2018). A key challenge is that many habitats exhibit considerable thermal heterogeneity (e.g. Milling et al. 2018), which can enable species to find shelter from short duration temperature extremes (Suggitt et al. 2011; Suggitt et al. 2018). Techniques to measure microclimate heterogeneity relative to the limits of species' tolerances are essential for predicting extinction risks of small-bodied species (Pincebourde et al. 2016; Potter et al. 2013; Rebaudo et al. 2016; Suggitt et al. 2018), but are likely to require emerging remote sensing technologies (Zellweger et al. 2019).

Unmanned aerial vehicles (UAVs, or drones) show considerable promise in ecological research (Christie et al. 2016; Duffy et al. 2021; Zellweger et al. 2019). The availability of powerful, lightweight sensors, including thermal, multispectral, visible light, and LiDAR, create opportunities to translate broad-scale models to particular habitats, which could help predict movements or presences of individual species within habitats (Anderson & Gaston 2013; Duffy

et al. 2021; Zellweger et al. 2019). Satellite thermal infrared (TIR) imagery and topographical data have been used in broad-scale ecological models (Zellweger et al. 2019). However, most satellite TIR imagery resolution is too coarse to detect and measure microclimates directly, particularly for small-bodied organisms, which may limit their application to air and soil microclimatic temperature measurements in some cases (Anderson & Gaston 2013; Zellweger et al. 2019). Radiometric thermal cameras mounted on UAVs provide measurements at very high resolutions that can complement broader-scale remote sensing measurements of temperature (Anderson & Gaston 2013; Brenner et al. 2018; Byerlay et al. 2020; Maes et al. 2017; Messina & Modica 2020; Milling et al. 2018). Prior to the onset of UAV and thermal camera technologies, microclimate studies required temperature loggers, such as iButtons (George et al. 2015; Holden et al. 2011). Such loggers are vital for calibrating and validating thermal remote sensing observations, but remote sensing provides unique advantages in terms of synoptic environmental measurement that greatly expands the reach of *in situ* ecological measurement (George et al. 2015; Holden et al. 2011; Kerr & Ostrovsky 2003).

The thermal limits of each species could predict the response of small-bodied species to climate change (Sunday et al. 2012). There is mounting evidence of species altering their historical range in response to habitats exceeding their thermal limitations (Hufnagel & Kocsis 2011; Soroye et al. 2020; Williams & Newbold 2021). When temperatures exceed a species' thermal tolerances, their fecundity and survival declines because they must expend energy on behavioural or physiological thermoregulation rather than resource gathering or reproduction (e.g. Buckley et al. 2021). The newly-developed and tested Thermal Position Index (~~TPI;~~ Kerr 2020; Soroye et al. 2020; Williams & Newbold 2021) relates species' realized thermal niches to their extinction-colonization dynamics. This method measures thermal tolerances using historical observations of air temperatures in areas where species have successfully persisted over time. Species' upper thermal limits evolve slowly, so adaptation rates are likely to be insufficient to permit many species to tolerate rapid warming (Araújo et al. 2013; Bennett et al. 2021).

This paper proposes a new methodological framework to measure landscape-scale microclimatic profiles with UAV and thermal infrared imaging technology, and illustrates their use in a practical conservation setting. We simultaneously outline a method of translating the Thermal Positioning Index, previously validated at global scales, to microclimatic applications. This framework includes five steps: data collection, assessment of species' thermal limits, map building, mapping of thermal conditions relative to species' measured tolerances, and interpretation (*sensu* Faye et al. in 2016). We present examples of how individual species' tolerances can be linked to remotely sensed thermal data to describe habitat suitability for three butterfly species: *Hesperia sassacus* (Indian skipper), *Speyeria aphrodite* (Aphrodite fritillary), and *Coenonympha tullia* (Common ringlet).

Materials & Methods

STEP 1 - DATA COLLECTION

Study Site. Field sites were located in Burnt Lands Provincial Park situated 30km west of Ottawa, ON, which hosts an alvar ecosystem interspersed with mostly coniferous tree stands. Fifteen sites of varying sizes separated by a minimum of 20 m of forested area were selected (Gordon & Kerr 2022). All sites consisted of open areas and clearings. Only two were not surrounded by trees. Research and UAV use permits were provided by Ontario Parks. Recognized as rare and imperiled ecosystems by the Nature Conservancy of Canada, alvars are characterized by open and barren areas with little to no soil, and often host rare species (NCC 2020). During summer, these landscapes can experience highly localized extreme heat in areas with exposed limestone, while vegetated areas nearby might have considerably lower temperatures. The spatial variability in these thermal conditions has not previously been measured.

UAV and Sensor. A DJI Matrice 300 quadcopter with real-time kinetic (RTK) positioning was deployed. This drone carried a Zenmuse XT2 dual sensor with thermal (13mm focal length; 640x512 image capture) and visual (8mm focal length, 12 megapixel resolution) imaging capabilities (DJI Inc., Shenzhen, China). A RTK base station was deployed in the field, which increased the positioning accuracy of the UAV by providing real-time differential corrections, and eliminated the need for ground control points. The quadcopter was equipped with the DJI pilot program, which included a mission function allowing execution of automated flight and camera control sequences. Imaging was acquired during missions programmed in the DJI pilot program using satellite imagery. The thermal camera captured images in the thermal infrared (TIR) spectral range in the radiometric-jpeg (R-JPEG) format. Each pixel was embedded with temperature data. The in-camera emissivity value was set to 1 for TIR images and adjusted in the GIS workflow step outlined below. The visual camera captured images in the red, green, and blue spectral bands (RGB). Both cameras captured images simultaneously. Every image was geotagged with the RTK-corrected GPS coordinates.

Flight Plan. Image acquisition flight plans were programmed with a 90% image overlap on all sides to optimize mapping accuracy, as recommended by the Pix4DMapper software used in the mapping step (Pix4D SA, Lausanne, Switzerland). The UAV was programmed to capture images at 1 second intervals and fly at a constant 2.5 m/s speed to maximize survey area, given a 37-minute battery life limitation, while minimizing motion blur. All missions were performed at 37 meters altitude to achieve 5 cm thermal imaging resolution and 1 cm RGB imaging resolution. All flights were restricted to days above 15℃ with <50% cloud cover between 10:30am and 3:30pm to ensure the accuracy and comparability of the thermal imagery gathered (Dai et al. 1999). Cloud cover alters TIR-based temperature measurement, so all flight missions were paused during cloudy periods and resumed after they cleared. Missions were aborted if

conditions remained cloudy. Butterfly surveys were conducted in parallel to our UAV surveys. While the data was not used in this paper, the butterfly monitoring methodology's temporal and temperature requirements (i.e. between 10:45am and 3:45pm, and over 13℃) had to be respected for the drone surveys as well (Pollard 1977). As the method was designed for British summer conditions, mild liberties were taken with the methodology (i.e. earlier start but higher temperature requirement).

In situ Temperature Measurements. To calibrate temperature readings captured by the thermal imaging, temperature loggers were placed *in situ*. At each site, an iButton (DS1922L-F5#, Maxim, Dallas, USA; accuracy: ±0.5℃) coated in clear plastic (Roznik & Alford 2012) was placed on the ground approximately 1 meter into the tree line in full shade near each site's access point for convenience. The plastic coating provided a waterproofing barrier (Plasti Dip, Blaine, MN, USA) for the iButton but is not expected to significantly affect the air temperature readings in the shade (Roznik & Alford 2012). These temperature loggers (hereafter referred to as ground loggers) were assumed to measure near surface air temperature as tree shade blocked most solar radiation and acted as solar shields (Gies et al. 2007). Statistical verifications were made to support this assumption. Three ground loggers were lost in the field, likely due to wildlife interference. At three sites, three poles each containing three uncoated iButtons at 0.05 m, 0.75 m, and 1.5 m (total of 27 iButtons) were placed to record air temperature variations at different heights (Fig. 1). These poles were constructed out of white PVC pipes (Mittra et al. 2013). The three sites were chosen for their variation in dominant surface type (limestone, grass, and mix of both). Temperature loggers (hereafter referred to as pole loggers) were positioned on the tip of each protrusion and rest on wire mesh to allow ventilation. Additional holes were drilled along the main pole and on each protrusion to allow better ventilation. These temperature loggers were used to model the relationship between UAV captured remotely sensed soil surface temperatures and air temperatures as air temperature is the metric adult lepidopterans, our study group, are most exposed to. Every iButton was programmed to record temperature at 30-minute intervals and was placed in the field only to be retrieved at the end of the field season. Air temperature was also measured before every UAV mission in a shaded area using a handheld HT-86 humidity meter (Wal Front, USA; accuracy: ±0.5℃, ±3% RH).

STEP 2 - GENERATING THERMAL LIMITS

We extracted data on the five hottest and coldest locations in the ranges of butterfly species that were detected in our study sites based on a historical air temperature dataset (Harris et al. 2014). As in Soroye et al. (2020), we used a baseline observation period to estimate thermal limits. Only occurrences between 1901 and 1975 were considered when estimating species' upper and lower thermal limits. Climate change has accelerated rapidly after that baseline period. By using the location-month combinations, only the months where a species observation had occurred were considered to extract monthly maximum and minimum air temperatures. Therefore, the summer months of the overwintering sites would not be considered when

extracting thermal limits. Location-month combinations were used in lieu of location-day combinations due to lack of historical daily temperature data. These values have previously been shown to be informative with respect to insect and other species' vulnerabilities to changing frequencies of extreme weather (Outhwaite et al. 2022; Soroye et al. 2020; Williams & Newbold 2021). Historical air temperatures were obtained from the Climate Research Unit dataset (Harris et al. 2014). Lepidoptera occurrence information was extracted from the eButterfly citizen science program (Prudic et al. 2017) and from longer term butterfly observations assembled through the activities of systematists and biological surveyors (Soroye et al. 2018). Each species observation is traceable to a curated museum specimen or to a submitted observation that has been approved by a team of butterfly experts.

STEP 3 - MAPPING

A total of 30 drone surveys were conducted from May 17 to August 26, 2021. One survey was discarded due to a brief malfunction with the RTK base station, which caused georeferencing discrepancies. As a result, every raster output was produced 29 times for each of the drone surveys. Raw TIR and RGB images collected in the field were used to generate TIR, RGB, digital surface model (DSM), and digital terrain model (DTM) orthomosaics (i.e. a georeferenced aerial image geometrically corrected; Faye et al. 2016) using the Pix4Dmapper software. The software used the embedded GPS information in each image and detected characteristic objects in the images to generate tie points and create densified point clouds. These clouds were then used to blend overlapping images and create an orthomosaic (hereafter referred to as map) with the original pixel information still intact. For each of the 29 surveys, one map of each type (TIR, RGB, DSM, DTM) was created. TIR maps had an approximate resolution of 5 cm/pixel, while RGB, DSM, and DTM maps had an approximate resolution of 1 cm/pixel.

STEP 4 - GIS PROCESSING

Classified Surface Type Map. The RGB maps were then imported into ArcGIS Pro software (Esri, Redlands, CA, USA). Thermal cameras estimate soil temperature by measuring the amount of infrared energy being reflected from the ground (Madding 1999). However, each surface reflects, absorbs, and emits re-radiated light differently (i.e. emissivity). To better estimate soil surface temperature, correcting for surface emissivity is essential (Madding 1999). To correct the remotely sensed soil surface temperature TIR maps for emissivity, each RGB map had to be classified by surface type (Becker 1987; Faye et al. 2016). This was accomplished using the *Classification Wizard* tool. The following surface types were included in the classification schema: debris, forest, grass, tall grass, limestone, shrub, soil, water, and wood. An object-based classification type was used using a supervised classification method. In each RGB map, approximately 25% of each surface type was identified using the *Segment Picker* tool. This process generated a classified raster with each pixel identified as the appropriate surface type.

These maps were validated by matching ground truth data about major landscape features to the land cover classification.

Emissivity Map. To create emissivity rasters, an "Emissivity" field was added to the classified maps' attribute tables. The emissivity values were added manually based on a literature review (Table 1). Objects identified as debris were given an emissivity value of 1 as their composition was not always known. Each map was then resampled to match the pixel size of the classified maps to the pixel size of the thermal maps. The emissivity values were extracted into a new raster and turned into floating point rasters to ensure the emissivity map was in the same raster format as the TIR maps.

Emissivity-Corrected Remotely Sensed Soil Surface Temperature Map. Emissivity-corrected soil surface temperature maps were created by multiplying the TIR maps with the emissivity maps. The difference in focal length between the TIR and visual cameras caused occasional misalignments between the RGB and TIR maps. As such, the emissivity and TIR maps were first manually aligned.

Modelling Air Temperature. To transform the remotely sensed soil surface temperature maps into air temperature maps, we modelled the relationship between the air temperatures (ground and pole logger data) and soil surface temperatures (emissivity-corrected remotely sensed soil surface temperature maps) at a given position. We ensured air temperature data of different logger heights was not statistically different before performing the model. The mean temperature in a 30cm radius around the iButton locations were extracted and used as soil surface temperature proxy on the corrected soil surface temperature maps. The iButton temperature recorded nearest the time of the UAV survey was used as air temperature. A simple linear regression model with 76 data points was constructed in R to relate air temperature to remotely sensed soil surface temperature used here as the independent variable (R Core Team 2020). Although air temperature data recorded via iButtons was considered to represent "true" temperatures, it was used as the dependent variable. This allowed for an easier calibration of remotely sensed soil surface temperatures into air temperatures. As this regression model was statistically strong, we used the model slope's equation to calibrate drone-based ground temperature maps into air temperature measurements.

Soil surface temperatures differ greatly between shaded and open areas, primarily due to solar radiation. The effects of radiation on organismal body temperatures are complex, depending on factors such as behaviour, body size, and coloration (Stelbrink et al. 2019; Stevenson 1985). To avoid systemic biases due to variability in solar radiation, we limited UAV operation to cloud-free times around mid-day and treated radiation as a constant in our subsequent modelling (Dai et al. 1999). We opted to measure *in situ* air temperature in the shade, as convention dictates when measuring ambient air temperature, to find a single generalized conversion factor for soil surface to air temperature over our study sites. This methodology was

developed to require minimal microhabitat temperature modelling. Therefore, pole loggers were placed in sites with varying surface types to account for the landscape variability, and data were pooled together to generalize the model across the study sites. The resulting air temperature model remained statistically strong and facilitates its reproducibility in different ecosystems. A main objective of our study was to adapt a verified global index of species vulnerability to microclimatic scales. A big component of this index uses historical air temperature data captured from meteorological stations to estimate species thermal niche boundary. As such, air temperature measurements needed to be used to generate the ~~TPI~~, and overheating index of each species.

Air Temperature Map. Air temperature maps were extrapolated from the emissivity-corrected remotely sensed soil surface temperature maps using the aforementioned air temperature model equation (Fig. 2). These maps were used in step 5 (see below) as they better represent the thermal conditions experienced by animals and airborne insects such as *Lepidoptera*.

Thermal Positioning Map. Thermal positioning maps were generated using the historical thermal limits of the study species (*H. sassacus*, *S. aphrodite*, and *C. tullia*) and the air temperature maps. Thermal positioning maps estimate a species' proximity to its thermal limits in every pixel. These maps were estimated as

$$P = \frac{N_m - N_{Smin}}{N_{Smax} - N_{Smin}},$$

developed by Soroye, Newbold, and Kerr (2020), where P is the species' thermal position at a given location or pixel, N_{m} is the air temperature of a given pixel in the air temperature map, N_{Smax} is the species' upper thermal limit, and N_{Smin} is the species' lower thermal limit (Fig. 2). This index has previously been shown to predict extinction risk among bumblebees, aspects of population dynamics among mammals, and insect declines more generally (Kerr 2020; Outhwaite et al. 2022; Soroye et al. 2020; Williams & Newbold 2021; Williams et al. 2022). A value of 1 represents a pixel with a temperature value equal to the upper thermal limit. Values exceeding 1 represent pixels with temperature readings greater than the upper thermal limit of the species.

Canopy Height Map. Canopy height maps ~~(CHM)~~ were generated by subtracting the digital terrain maps from the digital surface maps. Terrain maps represent ground topography, while surface maps represent an elevation map of both natural and artificial features in addition to ground topography. The resulting ~~CHMs~~ represent the height of the natural and artificial features.

STEP 5 - ECOLOGICAL INDICES

Overheating Index. The overheating index was used as a landscape-scale relative heat indicator. It was calculated as the proportion of pixels within the UAV temperature measurement area where that species' thermal position was ≥ 1. For thermal position index, such values indicate that temperatures exceed the boundaries of that species' upper thermal limits.

Foliage Height Diversity. Foliage height diversity ~~(FHD)~~ represents the canopy height diversity and is used as a landscape heterogeneity index (MacArthur & MacArthur 1961). We classified canopy height maps to the nearest 0.5m interval and calculated the inverse Simpson index to assess this aspect of heterogeneity.

Thermal Diversity. Lastly, we assessed thermal diversity in a similar manner to foliage height diversity. First, we classified temperature data according to the nearest 0.5 ℃ temperature interval, and then calculated the standardized inverse Simpson index for each site (Faye et al. 2016; Fig. 3).

STUDY SPECIES

Butterflies were used as focal species. Butterflies are useful model organisms for small-scale climate change research (Beirão & Cardoso 2020). Due to their small size and dependence on temperature to regulate body heat, insects are considered good model organisms to predict species response to climate change (Beirão & Cardoso 2020; Wilson & Maclean 2011). However, few insect species have detailed contemporary and historical datasets like *Lepidoptera* (Wilson & Maclean 2011). As a result, the impact of climate change on butterflies has been well documented (Beirão & Cardoso 2020; Hufnagel & Kocsis 2011; Mattila et al. 2011; Wilson & Maclean 2011). We assessed thermal position indices for three butterfly species (*Hesperia sassacus*, *Speyeria aphrodite*, and *Coenoympha tullia*) that account for microclimatic variation at scales relevant to these species' individual movements and thermoregulation. These species were selected for their variation in body size, taxonomy, and thermal tolerance (5.40℃ to 28.56℃, -14.78℃ to 32.37℃, and -12.65℃ to 36.04℃ respectively). Each species was observed during transect based butterfly surveys. Beyond confirming the presence of our case study species at our study sites, results from these surveys are outside the scope of this paper.

Results

Foliage height diversity (which was log-transformed) exhibited a peaked relationship with thermal diversity ($R^2 = 0.1138$, $F(1,27) = 4.595$, $p = 0.04123$; Fig. 4). Visual inspection indicated that model residuals were normally distributed and homoscedastic.

Air temperature was measured at four different heights with iButton temperature loggers (0 m, 0.05 m, 0.75 m, 1.5 m) and related to air temperature measurements using an ANCOVA.

Temperature measurements did not differ statistically within this height range, so all air temperature measurements, regardless of height, were pooled for calibration and validation of remotely sensed soil surface temperature. Air temperature, as measured using *in situ* iButton instruments, related strongly to UAV-based remotely sensed temperatures ($R^2 = 0.7129$, $F(1,72) = 182.2$, $p << 10^{-4}$). Therefore, we used the resulting regression equation, $y = 0.5558x + 11.12999$, to calibrate air temperature values and map them (Fig.5).

Coarse air temperature was a significant predictor of the overheating index for *H. sassacus* ($R^2 = 0.2902$, $F(1,27) = 12.45$, $p = 0.0015$), *S. aphrodite* ($R^2 = 0.3058$, $F(1,27) = 13.34$, $p = 0.0011$), and *C. tullia* ($R^2 = 0.2396$, $F(1,27) = 9.825$, $p = 0.0041$). The overheating index position of our three example species diverged increasingly with increasing coarse air temperature (Fig. 6). Handheld humidity meter observations (which measure temperature and humidity) collected *in situ* were assumed to be a validated method of capturing locality-specific air temperature data, while drone-based temperature measurements provide the basis for the site-level metric of overheating and spatial heterogeneity in thermal position. Site level average overheating potential for these species relates to contemporary *in situ* temperature measurements (Figure 6). These *in situ* values are on the x axis as thermometer measurements of temperature should have very small errors relative to any other technique we employed, including remote sensing measures. Overheating indices for each species were not statistically related to thermal diversity or foliage height diversity.

Discussion

Here, we demonstrate the feasibility of direct, synoptic measurements of seasonal temperature extremes relative to individual species tolerances using a UAV-borne thermal sensor. Landscape heterogeneity relates strongly to variation in temperature extremes within habitats, relative to the limits of species' thermal tolerances (see also Carroll et al. 2016; Milling et al. 2018; Suggitt et al. 2018) that are known to affect insect species persistence at broader spatial extents (Soroye et al. 2020; Kerr 2020; Outhwaite et al. 2022). The method developed here complements temperature measurements that can be interpolated from coarse resolution remote sensing and from meteorological station data (Kearney et al. 2020; Maclean & Klinges 2021; Fig. 4). While previous work demonstrates that some insect species' extinction risks depend on the frequency and intensity of temperature extremes, as measured using the thermal position index (Soroye et al., 2020) or derivatives (Outhwaite et al. 2022), this is the first demonstration that these metrics can be assessed using remote sensing methods within individual habitats.

The importance of microclimatic variation and microclimatic refugia in protecting species from the growing risks of extreme weather has been demonstrated empirically (Bladon et al. 2020; Milling et al. 2018; Riddell et al. 2021). The foundations of such work rely on observed habitat characteristics (Bladon et al. 2020) and frequently employ coarse resolution remote

sensing imagery (Riddell et al. 2021) to estimate landscape heterogeneity relative to species' habitat use. Those techniques are essential for ongoing assessments of microclimatic refugia within habitats because they can provide broad coverage relative to higher resolution, but relatively localized, UAV-based measurements. Nevertheless, more detailed remote sensing at very high resolution (in this study, 5cm), provides accurate temperature measurements that demonstrate the extent and magnitude of thermal refugia that result from physical heterogeneity within particular habitat patches. These measurements are consistent with observations made at much broader spatial scales (Carroll et al. 2016; Suggitt et al. 2018), though previous work has not assessed microclimatic variation in the context of thermal position. As all survey sites were within the same landscape, and most were very similar in their landscape features, landscape heterogeneity results were very similar. Repeating this methodology in more varied physical landscapes and ecosystems would likely produce more diverse results (Carroll et al. 2016; Gies et al. 2007). We believe the approach we have described here represents a step toward assessing fine-grained thermal constraints in real-world habitats.

The overheating indices for the three study species (*H. sassacus*, *S. aphrodite*, and *C. tullia*; Fig. 2) highlighted the relative impact of localized temperature extremes on individual species relative to species' thermal limits. Variance in the within-habitat overheating index increased as temperatures rose for each of the three species for which thermal position index (and its spatial average, the overheating index) was measured, suggesting that microclimates persisted in these areas through the warmest periods we observed. As these microclimates depended on structural habitat heterogeneity (e.g. partial canopy cover and shrubs, for example), maintenance of these habitat characteristics and potentially the restoration or addition of those characteristics to habitats could improve species' resilience to warming conditions, even through the hottest periods observed within this region. Additional work is needed to assess how individual species' movements and persistence within and among these habitats might relate to thermal conditions, independent from other landscape characteristics, such as habitat connectivity.

Infrared imagery has frequently been used to study surface temperatures in agricultural and geological studies (Faye et al. 2016; Harvey et al. 2016; Maes & Steppe 2019; Sener et al. 2019). However, in ecological studies, air temperature is the primary metric for many species, including adult butterflies. Transformation of UAV-acquired soil surface temperature measurements into air temperature measurements is necessary to transform these remote sensing tools' outputs into measurements that have the greatest biological relevance for organisms, like butterflies, that spend relatively little time on exposed ground (though, we note that many butterfly species sometimes obtain nutrients from moisture on soil surfaces). Butterfly species are more likely to be vulnerable to surface temperature extremes during egg and larval phases of development (Pincebourde et al. 2021). It is likely to be possible to alter the framework we have applied here to measure temperatures most relevant to butterflies during those life stages, but

more work would be needed to understand temperature variability within the areas through which caterpillars moved as well as on the temperature dependence of ovipositioning behaviour of adult butterflies. Because *in situ* air temperature measurements matched remote sensing metrics quite closely (Fig. 5), we expect that UAV-based thermal measurements, especially if related to thermal tolerances of eggs and larvae, could inform risks of extreme temperatures for butterflies during these earlier life stages.

We found that air temperatures showed little variation from ground level to a height of 1.5 metres within the alvar habitats where we collected *in situ* temperature values. Our measurements were made over areas with vegetated ground cover, which might have reduced temperature variability over this small range. Limestone pavement surface temperatures can be extremely hot in this habitat. Our results would have differed had our ground surface temperatures focused on those areas. Butterflies were not observed to settle onto such surfaces during hot periods. Different habitat types may exhibit other relationships between ground and air temperatures than that observed here, depending on vegetation type, vegetation density, and solar radiance (Gies et al. 2007). Our results suggest species that must engage in behavioural or physiological thermoregulation in hot conditions may face challenges escaping extreme heat by moving upward along vegetated surfaces or adjusting flight heights during foraging. Instead, such species (including the study species) will likely need to rely on heterogeneity within the habitat to find localities where vegetation creates cooler temperatures from ground to canopy and to adjust their activity periods away from the hottest times of day. Disturbances in these habitats that create more homogeneous conditions, such as removing small patches of trees or shrubs, or perhaps even mowing, may eliminate critical thermal microrefugia (Larsen 2012), and reduce the likelihood of species' persistence. We predict such effects to become more pronounced as extreme temperatures become more frequent and severe. Remote sensing-based measurements of temperatures within particular habitats will be more relevant and reliable for conservation applications if calibrated by *in situ* temperature measurements. Calibration is necessary as UAV-based estimates of temperature, though strong ($R^2 = 0.7129$), tended to be slightly lower than *in situ* iButton measurements, perhaps owing to UAV thermal measurements integrating more variable air temperatures above ground level.

Estimates of the thermal position index focused on peak flight seasons for three butterfly species with divergent thermal tolerances. A more thorough estimate of the effects of temperature extremes on butterfly, or other species', biology would require temperature monitoring throughout the year. We do not discount the potential importance of microclimates at other times of year, but our main focus was on measuring thermal position of habitats during the warmest periods of butterfly activity. Consequently, repeated surveys at each site assessed different temperature regimes, separated by several weeks, which we treated as independent data points. Growing frequency and severity of extreme weather is expected to cause negative

population growth among many species, but local losses of species might require several years of such climate-driven declines.

Conclusions

Monitoring the biological impacts of extreme weather will require a broad array of remote sensing tools and techniques, ranging from broad-scale models drawing on coarse resolution remote sensing to UAV-based measurements that can directly observe within-habitat variation at scales relevant to site-level habitat management. Exposure to extreme temperatures that exceed species' tolerances increase their extinction risk across broad regions. This study demonstrates that such models can be translated to within-habitat scales, and identify microclimatic variability that is validated by *in situ* temperature measurements for individual species. We believe this work offers one avenue to expand monitoring efforts for biological diversity that can inform practical conservation management.

Acknowledgements

We thank Dr. Anders Knudby (University of Ottawa) and Dr. Scott Mitchell (Carleton University) for their early input on the project design and methodology. We also thank Dana Martin for her help with data collection and compilation.

References

Algar AC, Kharouba HM, Young ER, and Kerr JT. 2009. Predicting the future of species diversity: macroecological theory, climate change, and direct tests of alternate forecasting methods. *Ecography* 32: 22-33.

Anderson K, and Gaston KJ. 2013. Lightweight unmanned aerial vehicles will revolutionize spatial ecology. *Frontiers in Ecology and the Environment* 11:138-146.

Araújo MB, Ferri-Yáñez F, Bozinovic F, Marquet PA, Valladares F, and Chown SL. 2013. Heat freezes niche evolution. *Ecology letters* 16:1206-1219.

Ashcroft MB. 2010. Identifying refugia from climate change. Wiley Online Library.

Becker F. 1987. The impact of spectral emissivity on the measurement of land surface temperature from a satellite. *International Journal of Remote Sensing* 8:1509-1522.

Beirão MV, and Cardoso DC. 2020. Thermal tolerance of fruit-feeding butterflies (Lepidoptera: Nymphalidae) in contrasting mountaintop environments. *Insects* 11:278.

Bennett JM, Sunday J, Calosi P, Villalobos F, Martínez B, Molina-Venegas R, Araújo MB, Algar AC, Clusella-Trullas S, and Hawkins BA. 2021. The evolution of critical thermal limits of life on Earth. *Nature communications* 12:1-9.

Bladon AJ, Lewis M, Bladon EK, Buckton SJ, Corbett S, Ewing SR, Hayes MP, Hitchcock GE, Knock R, and Lucas C. 2020. How butterflies keep their cool: Physical and ecological traits influence thermoregulatory ability and population trends. *Journal of Animal Ecology* 89:2440-2450.

522 Brenner C, Zeeman M, Bernhardt M, and Schulz K. 2018. Estimation of evapotranspiration of
523 temperate grassland based on high-resolution thermal and visible range imagery from
524 unmanned aerial systems. *International Journal of Remote Sensing* 39:5141-5174.
525 Buckley LB, Schoville SD, and Williams CM. 2021. Shifts in the relative fitness contributions of
526 fecundity and survival in variable and changing environments. *Journal of Experimental*
527 *Biology* 224:jeb228031.
528 Byerlay RA, Nambiar MK, Nazem A, Nahian MR, Biglarbegian M, and Aliabadi AA. 2020.
529 Measurement of land surface temperature from oblique angle airborne thermal camera
530 observations. *International Journal of Remote Sensing* 41:3119-3146.
531 Carroll JM, Davis CA, Fuhlendorf SD, and Elmore RD. 2016. Landscape pattern is critical for
532 the moderation of thermal extremes. *Ecosphere* 7:e01403.
533 Christie KS, Gilbert SL, Brown CL, Hatfield M, and Hanson L. 2016. Unmanned aircraft
534 systems in wildlife research: current and future applications of a transformative
535 technology. *Frontiers in Ecology and the Environment* 14:241-251.
536 Dai A, Trenberth KE, and Karl TR. 1999. Effects of clouds, soil moisture, precipitation, and
537 water vapor on diurnal temperature range. *Journal of Climate* 12:2451-2473.
538 DJI. 2021. DJI Pilot (version v2.4.1.7). DJI Inc., Shenzhen, China.
539 Duffy JP, Anderson K, Fawcett D, Curtis RJ, and Maclean I. 2021. Drones provide spatial and
540 volumetric data to deliver new insights into microclimate modelling. *Landscape Ecology*
541 36:685-702.
542 Esri Inc. 2020. ArcGIS Pro (Version 2.5). Esri Inc, Redlands, CA, USA. Available at
543 https://www.esri.com/en-us/arcgis/products/arcgis-pro/overview.
544 Faye E, Rebaudo F, Yánez-Cajo D, Cauvy-Fraunié S, and Dangles O. 2016. A toolbox for
545 studying thermal heterogeneity across spatial scales: from unmanned aerial vehicle
546 imagery to landscape metrics. *Methods in Ecology and Evolution* 7:437-446.
547 George AD, Thompson III FR, and Faaborg J. 2015. Using LiDAR and remote microclimate
548 loggers to downscale near-surface air temperatures for site-level studies. *Remote sensing*
549 *letters* 6:924-932.
550 Gies P, Elix R, Lawry D, Gardner J, Hancock T, Cockerell S, Roy C, Javorniczky J, Henderson
551 S. 2007. Assessment of the UVR protection provided by different tree species.
552 *Photochemistry and photobiology* 83(6):1465-70.
553 Gilman SE, Wethey DS, and Helmuth B. 2006. Variation in the sensitivity of organismal body
554 temperature to climate change over local and geographic scales. *Proceedings of the*
555 *National Academy of Sciences* 103:9560-9565.
556 Gordon SC, Kerr JT. 2022. Floral diversity increases butterfly diversity in a multitrophic
557 metacommunity. *Ecology* e3735.
558 Harris IP, Jones PD, Osborn TJ, Lister DH. 2014. Updated high-resolution grids of monthly
559 climatic observations–the CRU TS3. 10 Dataset. *International journal of climatology*
560 34(3):623-42.
561 Harris RM, Beaumont LJ, Vance TR, Tozer CR, Remenyi TA, Perkins-Kirkpatrick SE, Mitchell
562 PJ, Nicotra A, McGregor S, and Andrew N. 2018. Biological responses to the press and
563 pulse of climate trends and extreme events. *Nature Climate Change* 8:579-587.
564 Harvey M, Rowland J, and Luketina K. 2016. Drone with thermal infrared camera provides high
565 resolution georeferenced imagery of the Waikite geothermal area, New Zealand. *Journal*
566 *of Volcanology and Geothermal Research* 325:61-69.

Helmuth B, Broitman BR, Yamane L, Gilman SE, Mach K, Mislan K, and Denny MW. 2010. Organismal climatology: analyzing environmental variability at scales relevant to physiological stress. *Journal of Experimental Biology* 213:995-1003.

Holden ZA, Abatzoglou JT, Luce CH, and Baggett LS. 2011. Empirical downscaling of daily minimum air temperature at very fine resolutions in complex terrain. *Agricultural and Forest Meteorology* 151:1066-1073.

Hufnagel L, and Kocsis M. 2011. Impacts of climate change on Lepidoptera species and communities. *Applied Ecology and Environmental Research* 9:43-72.

Kearney MR, Gillingham PK, Bramer I, Duffy JP, Maclean IM. 2020. A method for computing hourly, historical, terrain-corrected microclimate anywhere on Earth. *Methods in Ecology and Evolution* 11(1):38-43.

Keppel G, Van Niel KP, Wardell-Johnson GW, Yates CJ, Byrne M, Mucina L, Schut AG, Hopper SD, and Franklin SE. 2012. Refugia: identifying and understanding safe havens for biodiversity under climate change. *Global Ecology and Biogeography* 21:393-404.

Kerr JT. 2020. Racing against change: understanding dispersal and persistence to improve species' conservation prospects. *Proceedings of the Royal Society B* 287:20202061.

Kerr JT, Ostrovsky M. 2003. From space to species: ecological applications for remote sensing. *Trends in ecology & evolution* 18(6):299-305.

Kharouba HM, Algar AC, and Kerr JT. 2009. Historically calibrated predictions of butterfly species' range shift using global change as a pseudo-experiment. *Ecology* 90: 2213-2222.

Labed J, and Stoll M. 1991. Spatial variability of land surface emissivity in the thermal infrared band: spectral signature and effective surface temperature. *Remote Sensing of Environment* 38:1-17.

Larsen TH. 2012. Upslope range shifts of Andean dung beetles in response to deforestation: compounding and confounding effects of microclimatic change. Biotropica 44:82-89.

MacArthur RH, and MacArthur JW. 1961. On bird species diversity. *Ecology* 42:594-598.

Mackey B, Berry S, Hugh S, Ferrier S, Harwood TD, and Williams KJ. 2012. Ecosystem greenspots: identifying potential drought, fire, and climate-change micro-refuges. *Ecological Applications* 22:1852-1864.

Maclean IM, Klinges DH. 2021. Microclimc: A mechanistic model of above, below and within-canopy microclimate. *Ecological Modelling* 1;451:109567.

Madding RP. 1999. Emissivity measurement and temperature correction accuracy considerations. *In Thermosense XXI* Vol. 3700, pp. 393-401. International Society for Optics and Photonics.

Maes WH, Huete AR, and Steppe K. 2017. Optimizing the processing of UAV-based thermal imagery. *Remote Sensing* 9:476.

Maes WH, and Steppe K. 2019. Perspectives for remote sensing with unmanned aerial vehicles in precision agriculture. Trends in plant science 24:152-164.

Mattila N, Kaitala V, Komonen A, Päivinen J, and Kotiaho JS. 2011. Ecological correlates of distribution change and range shift in butterflies. *Insect Conservation and Diversity* 4:239-246.

Messina G, and Modica G. 2020. Applications of UAV thermal imagery in precision agriculture: State of the art and future research outlook. *Remote Sensing* 12:1491.

Milling CR, Rachlow JL, Olsoy PJ, Chappell MA, Johnson TR, Forbey JS, Shipley LA, and Thornton DH. 2018. Habitat structure modifies microclimate: An approach for mapping fine-scale thermal refuge. *Methods in Ecology and Evolution* 9:1648-1657.

613 Mineo S, and Pappalardo G. 2021. Rock emissivity measurement for infrared thermography
614 engineering geological applications. *Applied Sciences* 11:3773.
615 Mittra S, Etten Jv, and Franco T. 2013. Collecting weather data in the field with high spatial and
616 temporal resolution using iButtons.
617 Nature Conservancy Canada (NCC). 2020. Alvars 101. Available at
618 https://www.natureconservancy.ca/en/what-we-do/resource-centre/conservation-
619 101/alvars-101.html.
620 Nichol J. 2009. An emissivity modulation method for spatial enhancement of thermal satellite
621 images in urban heat island analysis. *Photogrammetric Engineering & Remote Sensing*
622 75:547-556.
623 Outhwaite CL, McCann P, Newbold T. 2022. Agriculture and climate change are reshaping
624 insect biodiversity worldwide. *Nature* 605(7908):97-102.
625 Pitarma R, Crisóstomo J, and Jorge L. 2016. Analysis of materials emissivity based on image
626 software. *New Advances in Information Systems and Technologies*: Springer, 749-757.
627 Pix4D. 2021. Pix4D Mapper. Pix4D SA, Lausanne, Switzerland. Available at
628 https://www.pix4d.com/.
629 Pincebourde S, Dillon ME, Woods HA. 2021. Body size determines the thermal coupling
630 between insects and plant surfaces. *Functional Ecology* 35(7):1424-36.
631 Pincebourde S, Murdock CC, Vickers M, Sears MW. 2016. Fine-scale microclimatic variation
632 can shape the responses of organisms to global change in both natural and urban
633 environments. *Integrative and Comparative Biology* 56(1):45-61.
634 Pollard E. 1977. A method for assessing changes in the abundance of butterflies. *Biological*
635 *conservation* 12(2):115-34.
636 Porfirio LL, Harris RM, Lefroy EC, Hugh S, Gould SF, Lee G, Bindoff NL, and Mackey B.
637 2014. Improving the use of species distribution models in conservation planning and
638 management under climate change. *PloS one* 9:e113749.
639 Potter KA, Arthur Woods H, Pincebourde S. 2013. Microclimatic challenges in global change
640 biology. *Global change biology* 19(10):2932-9.
641 Prudic KL, McFarland KP, Oliver JC, Hutchinson RA, Long EC, Kerr JT, and Larrivée M. 2017.
642 eButterfly: leveraging massive online citizen science for butterfly conservation. *Insects*
643 8:53.
644 Qin Z, Li W, and Gao M. 2006. Estimation of land surface emissivity for Landsat TM6 and its
645 application to Lingxian Region in north China. Remote Sensing for Environmental
646 Monitoring, GIS Applications, and Geology VI: SPIE. p 292-299.
647 R Core Team. 2019. R: A language and environment for statistical computing. R Foundation for
648 Statistical Computing, Vienna, Austria. Available at https://www.R-project.org/.
649 Rebaudo F, Faye E, and Dangles O. 2016. Microclimate data improve predictions of insect
650 abundance models based on calibrated spatiotemporal temperatures. *Frontiers in*
651 *physiology* 7:139.
652 Riddell E, Iknayan K, Hargrove L, Tremor S, Patton J, Ramirez R, Wolf B, and Beissinger S.
653 2021. Exposure to climate change drives stability or collapse of desert mammal and bird
654 communities. *Science* 371:633-636.
655 Roznik EA, and Alford RA. 2012. Does waterproofing Thermochron iButton dataloggers
656 influence temperature readings? *Journal of Thermal Biology* 37:260-264.
657 Rull V. 2009. Microrefugia. Wiley Online Library.

Sener M, Pehlivan M, Tekiner M, Ozden UE, Erdem T, Celen HH, Seren A, Aytac SA, Kolsuz HU, and Seyrek K. 2019. Monitoring of irrigation schemes by using thermal camera mounted UAVs. *Feb-fresenius environmental bulletin* :4684.

Slavich E, Warton DI, Ashcroft MB, Gollan JR, and Ramp D. 2014. Topoclimate versus macroclimate: how does climate mapping methodology affect species distribution models and climate change projections? *Diversity and Distributions* 20:952-963.

Sobrino JA, Jiménez-Muñoz JC, and Paolini L. 2004. Land surface temperature retrieval from LANDSAT TM 5. *Remote Sensing of Environment* 90:434-440.

Soroye P, Ahmed N, and Kerr JT. 2018. Opportunistic citizen science data transform understanding of species distributions, phenology, and diversity gradients for global change research. *Global Change Biology* 24: 5281-5291.

Soroye P, Newbold T, and Kerr J. 2020. Climate change contributes to widespread declines among bumble bees across continents. *Science* 367:685-688.

Stelbrink P, Pinkert S, Brunzel S, Kerr J, Wheat CW, Brandl R, Zeuss D. 2019. Colour lightness of butterfly assemblages across North America and Europe. *Scientific reports* 9(1):1-0.

Stevenson RD. 1985. Body size and limits to the daily range of body temperature in terrestrial ectotherms. *The American Naturalist* 125(1):102-17.

Suggitt AJ, Gillingham PK, Hill JK, Huntley B, Kunin WE, Roy DB, and Thomas CD. 2011. Habitat microclimates drive fine-scale variation in extreme temperatures. *Oikos* 120:1-8.

Suggitt AJ, Wilson RJ, Isaac NJ, Beale CM, Auffret AG, August T, Bennie JJ, Crick HQ, Duffield S, and Fox R. 2018. Extinction risk from climate change is reduced by microclimatic buffering. *Nature Climate Change* 8:713-717.

Sunday JM, Bates AE, and Dulvy NK. 2012. Thermal tolerance and the global redistribution of animals. *Nature Climate Change* 2:686-690.

Urban MC, Bocedi G, Hendry AP, Mihoub JB, Pe'er G, Singer A, Bridle JR, Crozier LG, De Meester L, Godsoe W, Gonzalez A. 2016. Improving the forecast for biodiversity under climate change. *Science* 353(6304):aad8466.

Van de Griend A, and OWE M. 1993. On the relationship between thermal emissivity and the normalized difference vegetation index for natural surfaces. *International Journal of Remote Sensing* 14:1119-1131.

Williams JJ, Freeman R, Spooner F, Newbold T. 2022. Vertebrate population trends are influenced by interactions between land use, climatic position, habitat loss and climate change. *Global change biology* 28(3):797-815.

Williams JJ, and Newbold T. 2021. Vertebrate responses to human land use are influenced by their proximity to climatic tolerance limits. *Diversity and Distributions* 27:1308-1323.

Williams SE, Shoo LP, Isaac JL, Hoffmann AA, and Langham G. 2008. Towards an integrated framework for assessing the vulnerability of species to climate change. *PLoS Biol* 6:e325.

Wilson RJ, and Maclean IM. 2011. Recent evidence for the climate change threat to Lepidoptera and other insects. *Journal of Insect Conservation* 15:259-268.

Zellweger F, De Frenne P, Lenoir J, Rocchini D, and Coomes D. 2019. Advances in microclimate ecology arising from remote sensing. *Trends in Ecology & Evolution* 34:327-341.

Table 1(on next page)

Emissivity values used for different land surfaces.

Surface Type	Emissivity	Source
Forest	0.99	Sobrino et al. 2004
Grass	0.98	Labed & Stoll 1991
Tall Grass	0.994	Labed & Stoll 1991
Limestone	0.95	Mineo & Pappalardo 2021
Shrub	0.986	Van de Griend & OWE 1993
Soil	0.95	Nichol 2009
Water	0.995	Qin et al. 2006
Wood	0.97	Pitarma et al. 2016

1

Figure 1

Image of a PVC pole containing iButtons at 0.05 m, 0.75 m, and 1.5 m deployed in the field.

Photo credit: Gabrielle Ednie.

Figure 2

Three temperature maps and three thermal positioning maps of a survey completed on August 3rd, 2021.

The maps were rendered slightly transparent and overlaid on a shaded relief map of its canopy height map to depict topographic variation also. The maps shown are as follows: (A) raw remote sensing temperature map, (B) emissivity-corrected remote sensing map, (C) air temperature map, (D) *C. tullia* thermal positioning map, (E) *S. aphrodite* thermal positioning map, and (F) *H. sassacus* thermal positioning map.

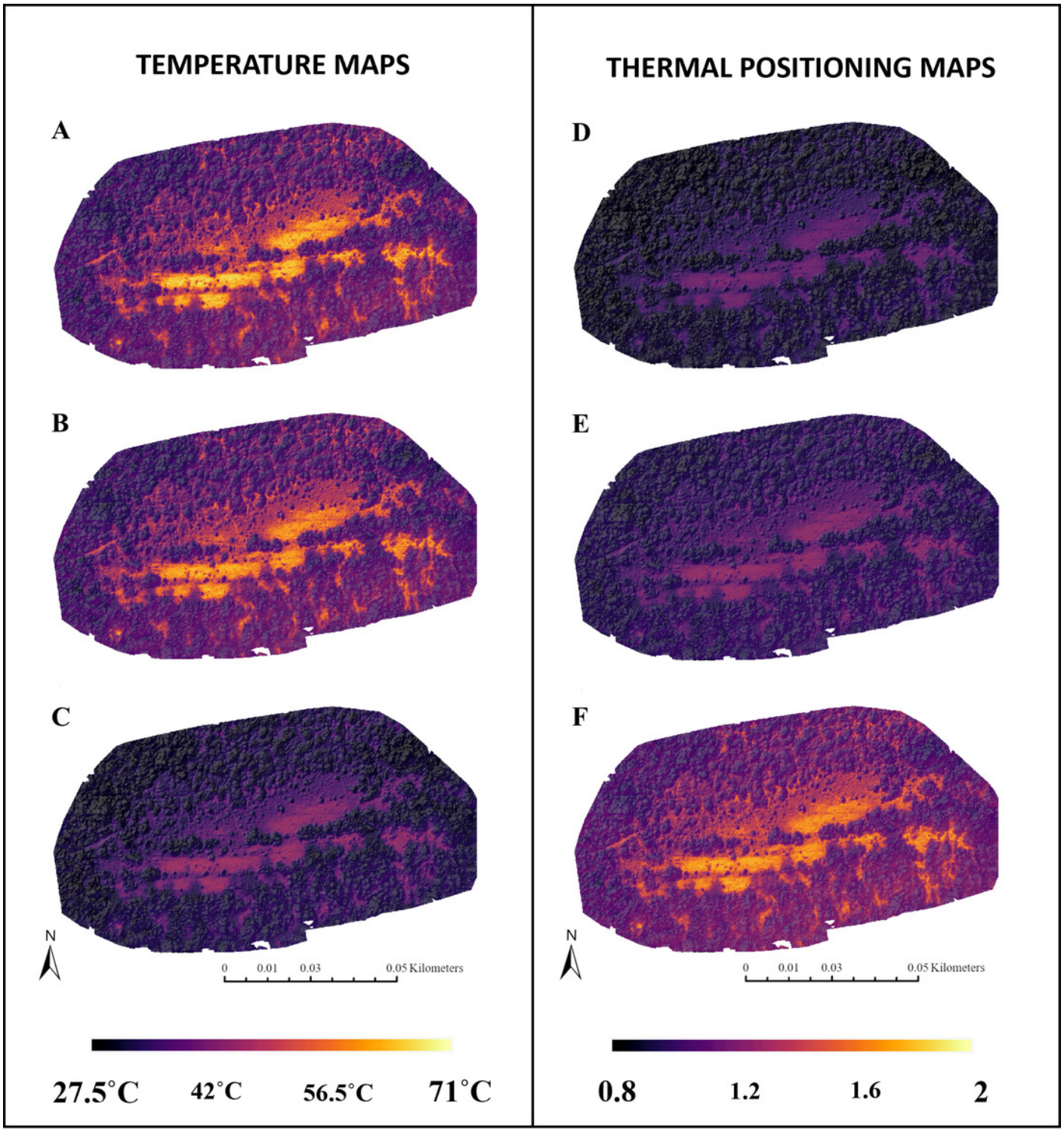
TEMPERATURE MAPS
THERMAL POSITIONING MAPS
A
B
C
D
E
F
N
0 0.01 0.03 0.05 Kilometers
27.5°C 42°C 56.5°C 71°C
0.8 1.2 1.6 2

Figure 3

Flowchart of the proposed methodological framework.

Dashed lines represent data from outside sources. Rectangular shapes represent intermediate outputs and steps. Oval shapes represent primary outputs from each step. All soil surface temperatures were remotely sensed.

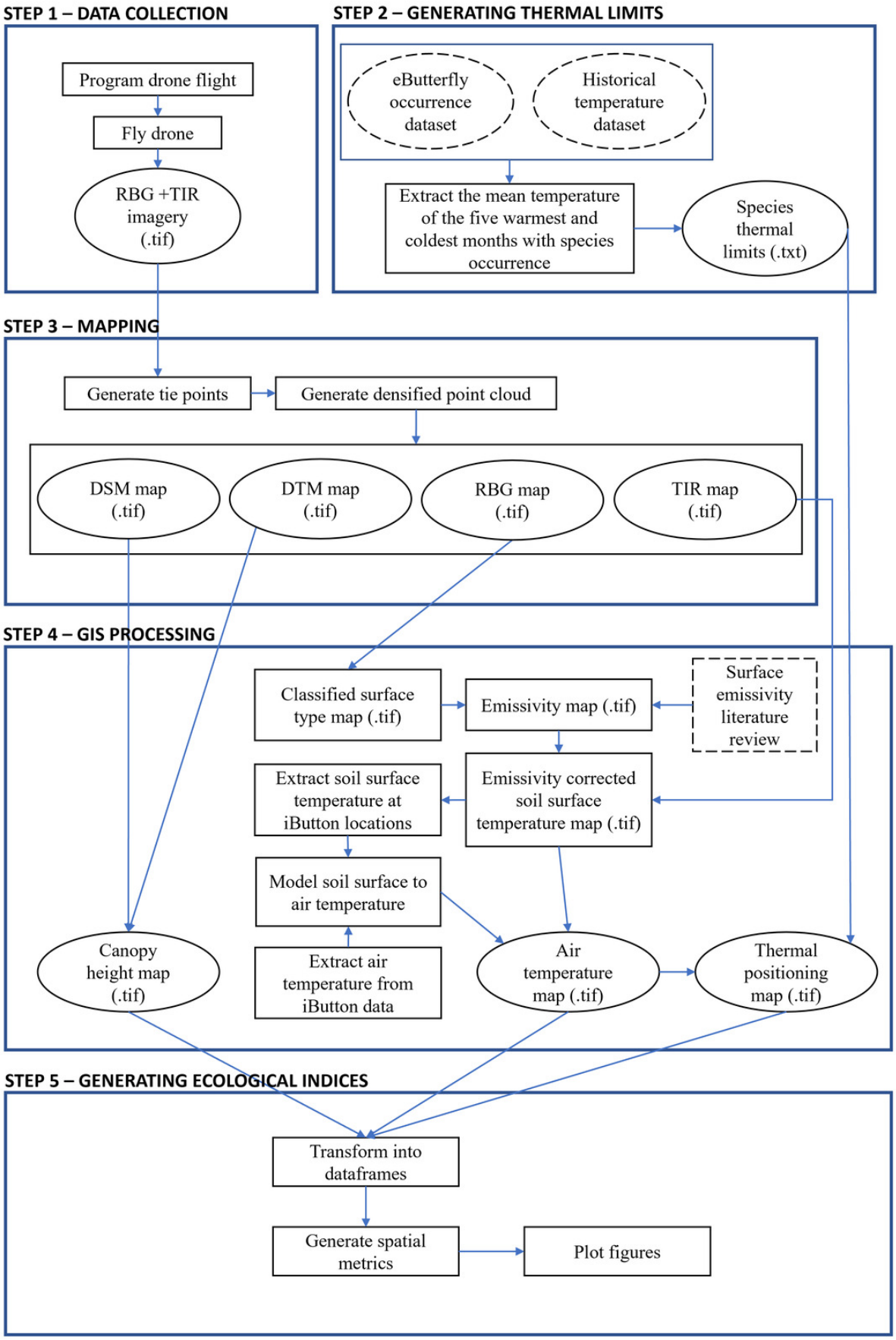
STEP 1 – DATA COLLECTION
Program drone flight
Fly drone
RBG +TIR imagery (.tif)
STEP 2 – GENERATING THERMAL LIMITS
eButterfly occurrence dataset
Historical temperature dataset
Extract the mean temperature of the five warmest and coldest months with species occurrence
Species thermal limits (.txt)
STEP 3 – MAPPING
Generate tie points
Generate densified point cloud
DSM map (.tif)
DTM map (.tif)
RBG map (.tif)
TIR map (.tif)
STEP 4 – GIS PROCESSING
Classified surface type map (.tif)
Emissivity map (.tif)
Surface emissivity literature review
Extract soil surface temperature at iButton locations
Emissivity corrected soil surface temperature map (.tif)
Model soil surface to air temperature
Canopy height map (.tif)
Extract air temperature from iButton data
Air temperature map (.tif)
Thermal positioning map (.tif)
STEP 5 – GENERATING ECOLOGICAL INDICES
Transform into dataframes
Generate spatial metrics
Plot figures

Figure 4

Plot of the relationship between the log of foliage height diversity and thermal diversity.

Each point represents one UAV survey.

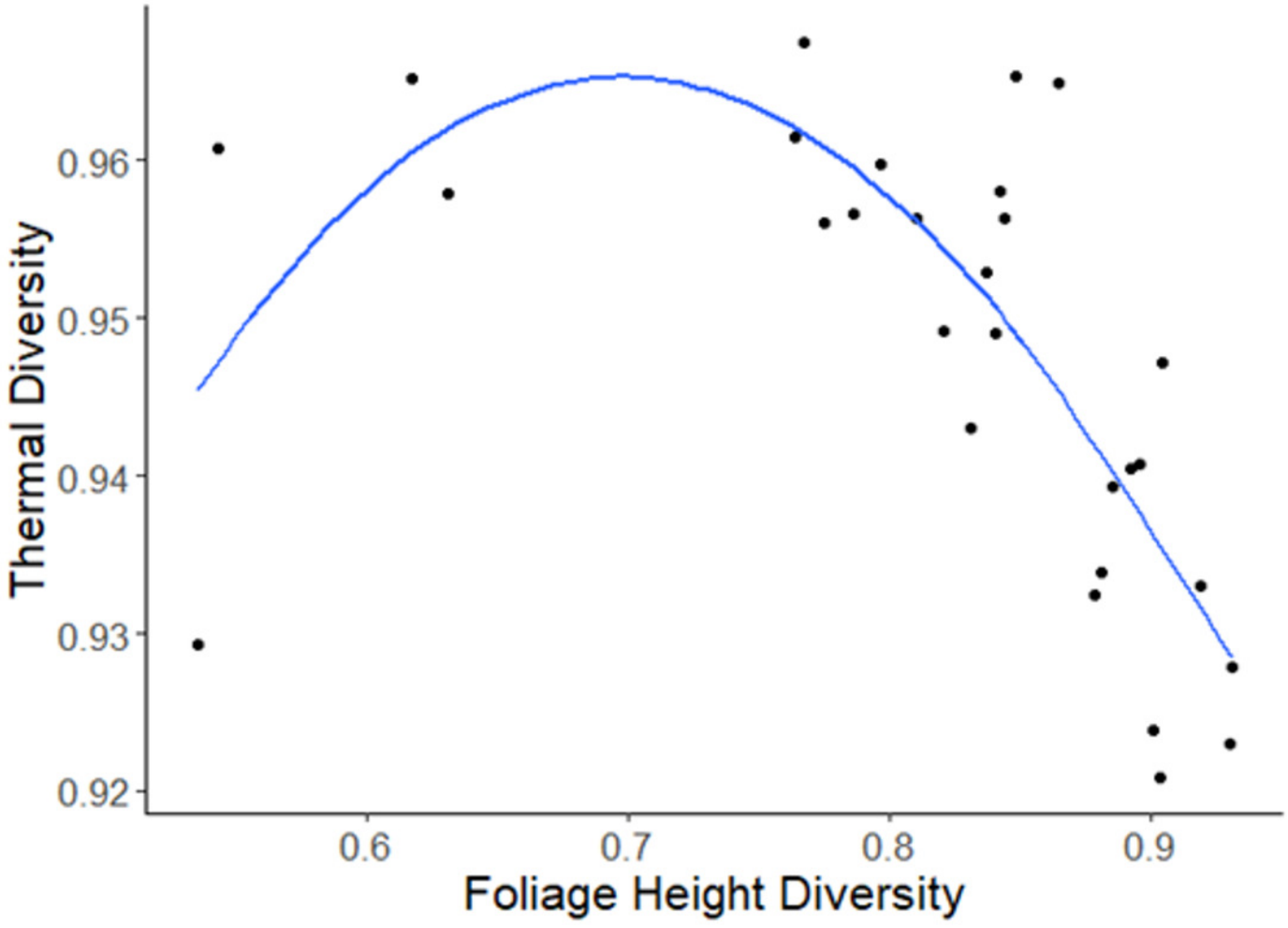

Figure 5

Relationship between remote sensing temperature and air temperature.

Remote sensing temperature was extracted from emissivity-corrected remote sensing temperature maps. Air temperature was extracted from *in situ* iButton temperature loggers launched in the study sites.

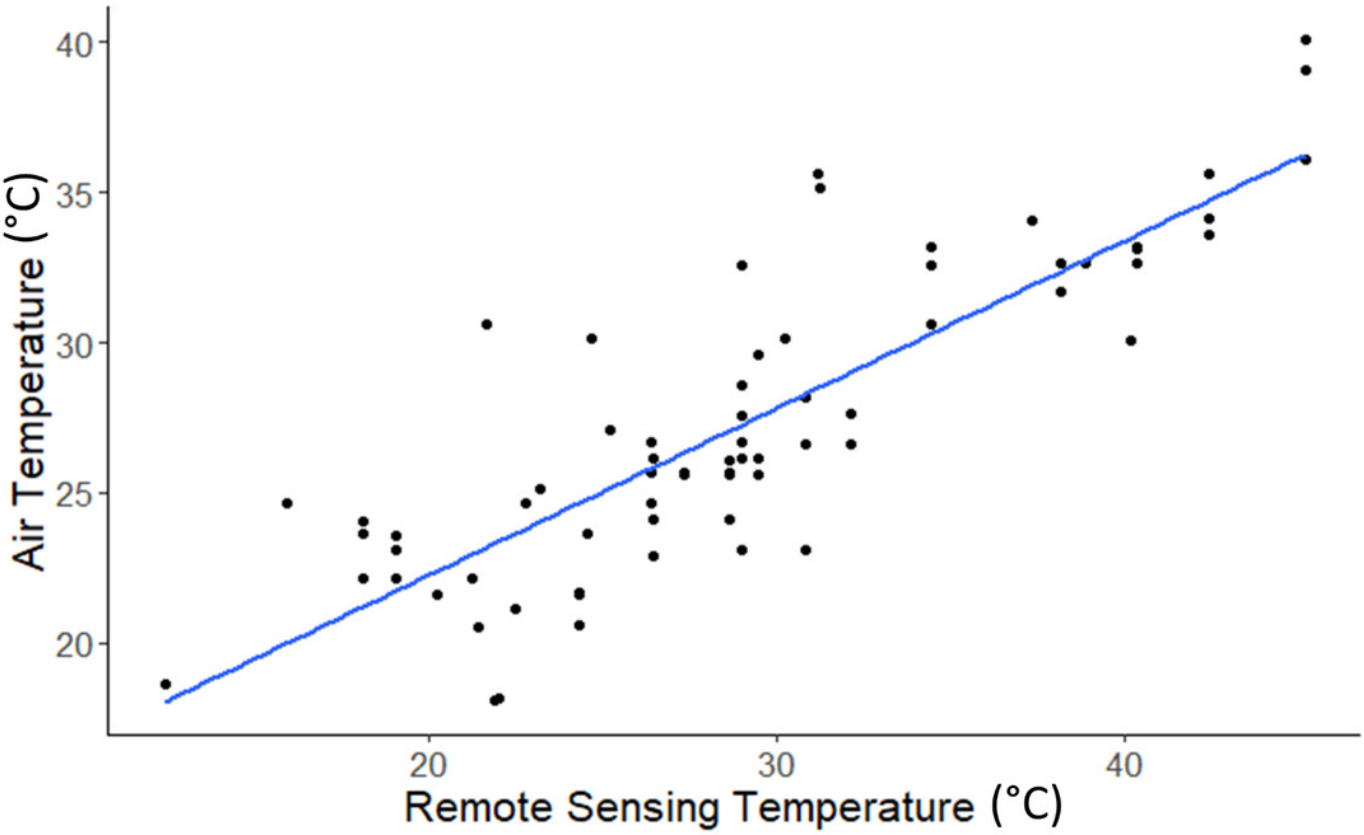

Figure 6

Plot of the overheating index of *H. sassacus*, *S. aphrodite*, and *C. tullia* in relation to coarse air temperature.

Coarse air temperature was measured using a handheld humidity meter at the time of each UAV survey.